Epigenetic EGFR gene repression confers sensitivity to therapeutic BRAFV600E blockade in colon neuroendocrine carcinomas

Jaume Capdevila[1], Oriol Arqués[2], Jose Ramón Hernández[3], Judit Matito[4], Ginevra Caratù[4], Francesco Mancuso[4], Stefania Landolfi[5], Jorge Barriuso[6], Paula Jimenez-Fonseca[7], Carlos Lopez[8], Rocio Garcia-Carbonero[9], Jorge Hernando[1], Ignacio Matos[10], Paolo Nuciforo[11], Javier Hernández[5], Manuel Esteller[3], Anna Martínez-Cardús[3], Josep Tabernero[1], Ana Vivancos*[4], Héctor G. Palmer*[2]

* Co-corresponding authors

Conflicts of interest

JC reports scientific consultancy role for Novartis, Pfizer, Ipsen, Bayer, Eisai, Sanofi and Merck Serono.

JB has received research funding from Pfizer, Novartis and Ipsen; consulting & advisory role for Pfizer, Novartis and Ipsen; travel accommodations and expenses from Pfizer, Novartis, AAA and Ipsen.

PJF has received funding from Pfizer for attending research meetings.

CL has received research funding from Pfizer, Novartis and Ipsen; consulting & advisory role for Pfizer, Novartis and Ipsen; travel accommodations and expenses from Pfizer, Novartis, AAA and Ipsen.

JT reports scientific consultancy role for Bayer, Boehringer Ingelheim, Chugai, Genentech, Inc., Ipsen, Lilly, MSD, Merck Serono, Merrimack, Merus, Novartis, Peptomyc, Pfizer, Rafael Pharmaceuticals, F. Hoffmann-La Roche Ltd, Sanofi, Symphogen and Taiho.

AV reports consultancy role for Sysmex, Merck and BMS.

HGP reports active collaborations funded by Bayern, MERUS, Blueprint and Cellestia.

The other authors declare no potential conflicts of interest.

[1] Medical Oncology Department, Vall d´Hebron University Hospital (HUVH). Vall d'Hebron Institute of Oncology (VHIO), Universitat Autònoma de Barcelona (UAB). CIBERONC. Barcelona, Spain.

[2] Stem Cells and Cancer Laboratory. Vall d'Hebron Institute of Oncology (VHIO). CIBERONC,

Barcelona, Spain.

[3]Cancer Epigenetics Group, Cancer Epigenetics and Biology Program (PEBC), Bellvitge Biomedical Research Institute (IDIBELL), Barcelona, Catalonia, Spain.

[4]Cancer Genomics Group. Vall d´Hebron Institute of Oncology (VHIO). Barcelona, Spain.

[5]Department of Pathology. Vall d´Hebron University Hospital (HUVH), Universitat Autònoma de Barcelona. CIBERONC, Barcelona, Spain.

[6]Department of Medical Oncology, European Neuroendocrine Tumor Society (ENETS) Centre of Excellence, The Christie NHS Foundation Trust. Division of Cancer Sciences, University of Manchester, Manchester, UK.

[7]Department of Medical Oncology, Central de Asturias University Hospital. Oviedo, Spain.

[8]Department of Medical Oncology, Marques de Valdecilla University Hospital. Santander, Spain.

[9]Department of Medical Oncology, Doce de Octubre University Hospital, Instituto de Investigacion Hospital 12 de Octubre (i+12), Centro Nacional de Investigacion Oncologica (CNIO). CIBERONC. Universidad Complutense de Madrid (UCM). Madrid, Spain.

[10]Early Clinical Drug Development Group. Medical Oncology Department, Vall d´Hebron University Hospital (HUVH). Vall d'Hebron Institute of Oncology (VHIO), Barcelona, Universitat Autònoma de Barcelona (UAB), Spain.

[11]Molecular Oncology Group. Vall d'Hebron Institute of Oncology (VHIO), Barcelona, Spain.

Corresponding author:
Héctor G. Palmer, PhD
Calle Natzaret, 115-117
Vall d´Hebron Institute of Oncology (VHIO)
08035 Barcelona, Spain
Tel: +34 932543450 (ext. 8649). Fax: +34 93 274 6708
hgpalmer@vhio.net

Corresponding author:
Ana Vivancos, PhD
Calle Natzaret, 115-117
Vall d´Hebron Institute of Oncology (VHIO)
08035 Barcelona, Spain
avivancos@vhio.net

ABSTRACT

Purpose: The limited knowledge of the molecular alterations that characterize poorly differentiated neuroendocrine carcinomas has limited the clinical development of targeted agents directed to driver mutations. Here we aim to identify new molecular targets in colon neuroendocrine carcinomas (co-NEC) and proof the efficacy of matching drugs.

Experimental Design: We performed a *multiomic* analysis of co-NEC to identify genetic or epigenetic alterations that could be exploited as effective drug targets. We compared co-NEC samples with colorectal carcinomas (CRC) to identify neuroendocrine specific traits. Patients with co-NEC and derived-xenografts (PDX) were treated with a BRAFV600E blocking drug to demonstrate sensitivity.

Results: co-NEC and CRC are similar in their mutational repertoire, although co-NECs are particularly enriched in *BRAFV600E* mutations. We report for the first time that *V600EBRAF* mutant colon neuroendocrine carcinomas may benefit from BRAF inhibition in monotherapy and how EGFR status is essential to predict innate sensitivity and acquired resistance by a differential methylation of its gene regulatory regions.

Conclusions: The identification of *V600E BRAF* mutations in high grade colon neuroendocrine carcinomas has allowed the description of radiological responses to combination therapy of BRAF and MEK inhibitors in basket clinical trials. However, the molecular rationale for this treatment combination was based on the presence of the BRAF mutation and the efficacy observed in other cancer types such as melanoma. Future drug development in this setting should test BRAF inhibitors upfront and the addition of anti-EGFR antibodies instead of MEK inhibitors for an efficient blockade of acquired resistance.

STATEMENT of SIGNIFICANCE

Targeting *BRAF* mutated cancers significantly differs between tumor types regarding sensitivity and resistance mechanisms. *EGFR* methylation status and its related protein expression is directly correlated with response and acquired resistance to BRAF inhibitors in colon neuroendocrine carcinomas that should impact in the future design of clinical trials in this setting.

INTRODUCTION

The low incidence and heterogeneity of neuroendocrine neoplasms has jeopardized their genomic profiling and thus the clinical development of targeted drugs directed to driver mutations. Fortunately, the molecular alterations driving carcinogenesis in neuroendocrine tumors are being revealed in the recent years.

Efforts have been focused in most prevalent neuroendocrine tumors, including pancreatic, small intestine and bronchopulmonary. Exome sequencing of pancreatic well-moderately differentiated tumors (European Neuroendocrine Tumor Society (ENETS)/World Health Organization (WHO) grade 1/2) showed alterations in three main pathways: DAXX-ATRX (death-domain associated protein-alpha thalassemia/mental retardation syndrome X-linked), MEN1 (multiple endocrine neoplasia) and mTOR (mammalian target of rapamycin)[1]. Contrarily, an equivalent genetic study on small intestine neuroendocrine grade 1/2 neoplasms described alterations in a large variety of oncogenic pathways[2]. A more recent study integrating exome sequencing, methylome and whole gene expression data catalogued small intestine grade 1/2 neuroendocrine neoplasms in three biological subtypes with different prognosis[3]. Finally, a similar multi-omic study on bronchopulmonary well-moderately differentiated neuroendocrine neoplasms (typical and atypical lung carcinoids) also demonstrated the existence of significant differences between low and high grade tumors, suggesting a distinct cell of origin[4].

Less frequent gastroenteropancreatic neuroendocrine tumors, such as high grade (ENETS/WHO grade 3) neuroendocrine carcinomas (NECs) are significantly less studied. This is not only due to their low incidence, but also to their poor prognosis and aggressive behavior leading to a low prevalence of advanced disease. Similarly to neuroendocrine small cell lung cancer[5], Gastroenteropancreatic NECs are systemically managed with treatments based on platinum chemotherapy following their histopathological characteristics. Unfortunately, Gastroenteropancreatic NECs show lower response to these standard treatments most probably due to a distinctive repertoire of molecular aberrations. Again, the lack of a detailed molecular profiling of these tumors has prevented the development of more effective target-directed therapies.

A recent study reported two *BRAF*^{V600E} mutant cases with metastatic high-grade rectal NEC that progressed to standard chemotherapy and later responded to the BRAF inhibitor dabrafenib combined with the MEK inhibitor trametinib[6]. This was an enlightening study that encouraged the identification of new drug targets by a further molecular characterization of intestinal NECs. This would be the first step to design new matched therapies that could be effective in patients refractory to standard-of-care chemotherapies.

In response, we performed a multi-omic study of a cohort of advanced colon NECs (co-NECs). We first observed a significant frequency of *BRAF*^{V600E} oncogenic mutations (28%). This result positioned co-NEC as the second tumor type most frequently mutated for *BRAF*, between melanoma (50%) and colorectal cancer (CRC) (15%) as described by the Genome Atlas Consortium (TCGA). Interestingly, a significant proportion of melanomas are sensitive to single agents blocking *BRAF*^{V600E} mutations whereas CRC tumors are not. It has been described that CRC tumors present high expression of EGFR as an alternative activation of MEK oncogenic pathway and a mechanism of resistance to *BRAF*^{V600E} inhibition[7]. Contrarily, EGFR expression is repressed by gene methylation in melanomas and thus they respond to single *BRAF*^{V600E} blockade[8]. This data suggests that despite co-NEC are tumors of the intestine as CRC, they may resemble more to melanomas regarding to their response to *BRAF*^{V600E} inhibitors. A more detailed characterization of co-NECs molecular traits and in particular the status of its EGFR/BRAF/MEK oncogenic pathway was crucial to understand the determinants of response to new target-directed drugs.

We profiled the mutations present in a panel of cancer-related genes and the methylome of a group of co-NECs and compared them to CRC cases. We observed that both tumor types show a similar mutational landscape with frequent mutations in *TP53, APC, KRAS* or *BRAF* genes. However, they presented a distinct methylome, suggesting a different gene expression profile and biological behavior. Indeed, *EGFR* gene was methylated in co-NECs in similar manner than in melanoma cases whereas in CRC was not. This hypermethylation correlated with lower EGFR expression in co-NEC. Furthermore, a Co-NEC Patient-derived Xenograft (PDX) model showed much higher sensitivity to a *BRAF*^{V600E} inhibitor alone than CRC PDXs. In addition, we show a case of a co-NEC patient with a *BRAF*^{V600E} mutation that responded to dabrafenib monotherapy, similarly to melanoma cases. She later progressed to treatment by increasing EGFR expression, suggesting a mechanism of resistance in co-NEC resembling that observed in CRC.

In summary, our results help to better understand the nature of co-NECs, allowing to design more precise and effective therapies targeting their molecular vulnerabilities and predict new potential mechanisms of resistance.

MATERIALS and METHODS

Study approval. Studies were conducted in accordance with the International Ethical Guidelines for Biomedical Research Involving Human Subjects. Human tumor samples for histological and molecular analyses and PDX were obtained after approval from the Ethics Committee of the Vall d'Hebron University Hospital [approval ID, PR(IR)79/2009]. Written

informed consent was signed by all patients. Experiments with mice were conducted following the European Union's animal care directive (86/609/CEE) and were approved by the Ethical Committee of Animal Experimentation of the Vall d'Hebron Research Institute (approval ID, 40/08 CEEA, 47/08 CEEA, 06/12 CEEA, 87/12 CEEA, 17/15 CEEA, and 18/15 CEEA).

Patient recruitment

Within the Spanish Task Force for Neuroendocrine and Endocrine Tumors (GETNE) national platform, 25 formalin-fixed and paraffin-embedded primary tumor samples of untreated patients with high-grade (ENETS/WHO grade 3), poorly differentiated NECs of colon origin (excluding rectum) were identified. All patients included in the study signed the informed consent form of the national database of the GETNE group (RGETNE) which standard operating procedures were approved by a National Scientific and Ethics Committee (PR(AG)82/2015). A referral expert pathologist in neuroendocrine neoplasms field confirmed the ENETS/WHO classification of the 25 tumor samples before starting molecular analyses. All tumors samples that underwent molecular analyses were defined as poorly differentiated grade 3 NECs, with Ki67 index >20% and/or >20 mitoses/10 high power fields (HPF).

Genomic analysis

Selection of tumor enriched tissue was performed with a cutoff >30% of tumor cells. Lymphocyte infiltration was determined. DNA was obtained and quality assessed by a qPCR-based method. The working method consisted of extraction of DNA tumor samples in formalin-fixed, paraffin-embedded tissue using the Maxwell 16 instrument (Promega®), followed by whole genome amplification (Decline-g, Qiagen®) in case of obtaining <600 ng. At least 600 ng of DNA is required to perform the mutational profiling using mutational VHIOCard. VHIOCard panel was designed in the laboratory of Cancer Genomics (Vall Hebron Institute of Oncology, VHIO) to analyze somatic mutations frequently observed in a broad panel of solid tumors, including neuroendocrine neoplasms (based on the COSMIC database: http://www.sanger.ac.uk/genetics/CGP/cosmic/). VHIOCard allows genotyping up to 700 mutations and small indels in 61 genes related to cancer (Supplementary table 1). Briefly, after the quantification (Nanodrop) and a dilution of genomic DNA to 10 ng/ml, a polymerase chain reaction (PCR) is performed to amplify genomic regions that are adjacent to loci genotyped (5-ml volume containing 0.1 units Taqpolymerase 20 ng of genomic DNA, 2.5 pmol of each "first" PCR and 2.5 mmol dNTPs triphosphate, dNTPs). The amplification reaction was carried out in a thermocycler. The unincorporated dNTPs are deactivated with the addition of alkaline phosphatase (0.3 U) and incubation for 40 minutes at 37ºC followed by heat inactivation of the

enzyme 5 minutes at 85ºC. After that, each mutation is analyzed as a product extension of one base (dNTPs are used in the presence of Taq polymerase) of a probe that hybrids immediately adjacent to the mutation position. After adding a cation exchange resin to remove residual salts from the reaction, 7nl of the matrix extension product are deposited (3-hidroxipicoloinic acid) on a SpectroCHIP Gen II chip (Sequenom). The Gen II SpectroCHIPs are analyzed using a mass spectrometer (matrix assisted Laser Desorption/Ionization-Time of Flight (MALDI-TOF) mass Spectrometer (MassARRAY, Sequenom).

Mismatch repair status

The status of mismatch repair activity was analyzed by immunohistochemistry (IHC) to detect repair proteins and polymerase chain reaction (PCR) to evaluate microsatellite instability (MSI). IHC was performed for MLH1 (G219-1129 clon, BD PharMingen Biosciences), MSH2 (G168-728 clon, BD PharMingen Biosciences), MSH6/GTBP (44 clon, BD PharMingen Biosciences) and PMS2 (A16-4 clon, BD PharMingen Biosciences). For MSI analysis we first used a DNA tissue extraction kit (Qiagen®) and then a Promega® system to evaluate by PCR the status of several microsatellites: BAT25, BAT26, NR-21, NR-24 and MONO-27.

DNA methylation analyses

DNA and methylation quality analyses identified 19 out of the 25 Co-NEC samples suitable for methylation study. The DNA extraction was performed using the "Infinium HD DNA FFPE Restoration" kit (Illumina®) ensuring adequate quality of genetic material. Bisulfite conversion was performed according to the manufacturer's recommendations for the Illumina® Infinium Assay. TheCo-NEC DNA was then hybridized using the Illumina® Infinium MethylationEPIC BeadChip arrays, which quantifies methylation of more than 850,000 CpG (5'-cytosine-phosphate-guanine-3') sites, covering 99% of the Reference Sequence (RefSeq) genes. The obtained data was jointly analyzed and compared with that already available in the TCGA database (http://cancergenome.nih.gov/) for 30 colorectal adenocarcinoma samples previously hybridized with the former HM450K Illumina® array, reporting methylation status for more than 450,000 CpG sites. Signal background and interplate variations were removed and normalized (standard GenomeStudio normalization) using internal control probes. Probes with a detection p-value >0.01 or without signal in one or more of the analyzed samples were also excluded as well as the ones containing a SNP (within the interrogation or extension bases), potentially cross-reactive or mapping to the sex chromosomes. Methylation differences between CRC adenocarcinomas and co-NECs tumors were identified through two-tailed unpaired F-tests correcting then for multiple comparisons ($p<2.55e-6$ for statistical

significance after correction). Most representative genes between the two neoplasms were identified from its content of significantly differentially methylated related CpGs.

Genes with CpG islands differentially methylated at their transcriptional start site (TSS200/TSS1500) were interrogated by Gene Set Enrichment Analyses (GSEA) using Broad Institute online tools. Additionally, leading-edge analysis were performed using GSEABase package in R. The leading-edge subset of genes are those genes that accounts for a specific gene set enrichment signal. The overlap between leading-edge genes in different oncogenic pathways were represented using ggplot2 R package. For multiple GSEA plots representation we used clusterProfiler R package[9].

Reverse transcription and quantitative PCR (qPCR)

To analyze *EGFR* gene expression by qPCR, RNA from tumor samples was extracted and used to synthesize cDNA using TRIzol™ (ThermoFisher Scientific) and iScript™ cDNA Synthesis Kit (Bio-Rad) respectively. A 7900HT qPCR System was used with Power SYBR-Green (Applied Biosystems). Relative gene expression was determined by the comparative CT method[10]. Primers used: Fw-*TATTGATCGGGAGAGCCGGA*, Rev-*TCGTGCCTTGGCAAACTTTC*.

Patient-derived xenograf (PDX) experiments

Animal experiments were conducted following the European Union's animal care directive (2010/63/EU) and were approved by the Ethical Committee of Animal Experimentation of VHIR (Vall Hebron Institute of Research –ID: 40/08 CEEA and 47/08/10). NOD/SCID (NOD.CB17-*Prkdc*^{scid}/NcrCrl) mice were purchased from Charles River Laboratories. 1x10^5 patient-derived cells suspended in PBS were mixed with Matrigel® (1:1 v/v-ratio; BD Biosciences) and injected subcutaneously into both flanks of NOD/SCID mice. When the tumor reached 0.5 cm^3 in volume, mice were randomized into different groups of treatment: vehicle, encorafenib (20mg/kg) and/or cetuximab (20 mg/kg). Cetuximab was administered by intraperitoneal injection twice per week and encorafenib diluted in 1% Tween 80 and 1% carboxymethyl cellulose and administered by oral gavage once a day. When matching end-point criteria mice were euthanized and complete necropsies were performed. Subcutaneous tumors were collected for histological analysis. A sample of each tumor xenograft was frozen in liquid nitrogen immediately after the extraction and kept at -80 ºC.

RESULTS

Genomic profiling of co-NECs

We selected tumor samples from 25 primary colon NECs from untreated patients. We first sequenced the coding region of 61 cancer-related genes in all cases (Supplementary table 1). The frequency of mutations per gene was compared to that described by TCGA in CRC (Figure 1 and Supplementary table 2). In general, all genes frequently mutated in CRC were also altered in Co-NECs, however some differences were observed. *TP53* and *BRAF* were more frequently mutated in co-NECs whereas *KRAS* was similarly altered. *APC* mutations were less frequent in co-NECs mostly due to the fact that not all its coding region was sequenced by our panel (Supplementary Table 1), whereas data from TCGA on CRC represented full exome sequencing. *SMAD4* gene was also mutated at lower frequency in co-NEC than in CRC despite all coding sequence was analyzed. Finally, a group of genes were mutated at a low frequency in in both co-NEC and CRC tumors. 24 out of these 25 tumors were evaluated for mismatch repair proficiency, all showing a preserved expression of DNA repair proteins and stable microsatellites.

Effective targeting of BRAFV600E in co-NEC

7 out of 25 Co-NECs presented *BRAF* mutations and 6 of them a *V600E* oncogenic alteration. This represented a 28% of co-NEC, that was higher than the 15,86% observed in CRC, and the only mutation targetable with available drugs such as dabrafenib or encorafenib. We therefore tested the potential efficacy of encorafenib on a PDX model derived from a liver metastasis of a patient with a co-NEC presenting a $BRAF^{V600E}$ mutation and stable microsatellites (Figure 2A). Encorafenib completely blocked tumor growth in contrast with its lack of effect on a PDX model derived from a liver metastasis of a patient with a CRC also presenting a $BRAF^{V600E}$ mutation and stable microsatellites (Figure 2A, B). In consequence, we decided to enroll a patient with a co-NEC presenting a liver metastases with a $BRAF^{V600E}$ mutation (Figure 2C) in an available clinical trial with another specific $BRAF^{V600E}$ inhibitor such as dabrafenib. Again, we observed a significant response to treatment (Figure 2E) despite her previous progression to standard-of-care treatment with cisplatin-etoposide chemotherapy combination.

Co-NEC present a distinctive methylome

Both CRC and co-NEC PDX models showed a completely different response to BRAF blockade despite presenting the same $BRAF^{V600E}$ targetable mutation, stable microsatellites and being derived from a liver metastasis. To further investigate the biological reason for such distinctive responses, we decided to define the methylome of co-NECs and compare it to CRC.

We obtained high quality DNA methylation analyses of 19 out of the 25 original co-NECs. We obtained excellent lecture quality in 391.474 CpGs positions, which were compared with TCGA data of CRC adenocarcinomas (Supplementary Table 3). Statistically significant differences ($p<2.55e-6$) were observed in 16.35% of CpGs, with an enrichment on regions related with gene expression promoters (TSS200 and 5´UTR) that generally showed less methylation in co-NEC than in CRC cases. This methylome profiling permitted to distinguish co-NECs from CRC adenocarcinomas as a different cluster of samples (Figure 3A, 3B, 3C). All these significant methylome differences confirmed that we were facing two biologically distinct types of intestinal tumors.

Indeed, we observed that genes such as somatostatin and other neurotransmitters, typically expressed in neuroendocrine cells, were higher methylated in CRC adenocarcinomas than in co-NECs or even melanoma samples (Supplementary Figure 1). This data may suggest that co-NEC preserved a methylome inherited from a different cell of origin than the epithelial progenitors of CRC adenocarcinomas.

We also observed that genes differentially methylated in co-NEC versus CRC adenocarcinomas were related to a variety of biological processes such as immune cell differentiation, cytoskeleton dynamics and cell polarity, DNA damage or apoptosis (Figure 3D, 3E). Future studies are required to evaluate the biological relevance of particular genes or gene sets presenting this methylation status distinctive of co-NECs.

EGFR gene is repressed by methylation in co-NEC

Considering these particularities of the co-NEC methylome and the relevance of high *EGFR* expression conferring resistance to $BRAF^{V600E}$ blockade[7], we evaluated in detail its gene methylation status. We observed that *EGFR* gene presented two sites with a higher methylation in co-NECs than in CRC (Figure 4A). These same sites were previously described to be higher methylated in melanomas[8]. Indeed, histological evaluation of EGFR expression revealed a lower expression in co-NEC than in CRC adenocarcinomas (Figure 4B and 4C). We also observed that EGFR protein was almost absent in cancer cells of the liver metastasis in a patient prior entering a clinical trial with dabrafenib, and it was clearly increased upon progression to $BRAF^{V600E}$ inhibition (Figure 2C-E, 4D and 4E).

Altogether this data indicated that in co-NECs, methylation of *EGFR* gene lead to its gene repression allowing a therapeutic response to $BRAF^{V600E}$ inhibition. Similarly to CRC adenocarcinomas presenting low *EGFR* methylation and innate high gene expression, a co-NEC resistant to $BRAF^{V600E}$ inhibition increased EGFR expression as a potential mechanism of acquired resistance.

We further confirmed that EGFR signaling was not relevant in a *BRAF*^{V600E} co-NEC PDX model since its blockade by cetuximab did not added any benefit when combined with dabrafenib (Figure 2A, 2B, 4F). In contrast, cetuximab further reduced tumor xenograft growth of a *BRAF*^{V600E} CRC PDX when combined with dabrafenib. This innate differential response to single and combined treatments is in line with the lower expression of EGFR protein in the co-NEC PDX than in the CRC PDX model (Figure 4G and 4H).

DISCUSSION

Colon NECs represent a group of neuroendocrine neoplasms with high aggressiveness and poor prognosis with very limited treatment options. The standard therapy derives from its histological similarities with small-cell lung cancer, another high-grade neuroendocrine carcinoma. However, results with platinum and etoposide in NECs of the digestive system are significantly inferior, suggesting important biological differences between both types of NECs. Other chemotherapies such as FOLFOXIRI are showing slightly better results than platinum-etoposide in co-NEC.

Co-NECs are a rare entity which molecular characteristics are not well defined. Here we present the most comprehensive molecular and translational analyses of co-NECs currently reported. From genomics perspective, we observed a similar gene mutational profile compared with CRC. However, the percentage of mutated cases per each cancer-related gene was significantly different in both tumors types. Interestingly, co-NECs showed a similar mutation profile than non-hypermutated CRC tumors with the involvement of *TP53*, *APC* and *KRAS*. However, the high percentage of *BRAF*^{V600E} mutations (28%) found in co-NECs was more similar to MSI hypermutated CRC (47%). We have not identified MSI in co-NECs suggesting chromosomal instability instead of mismatch repair deficiency as the main source of genetic alterations.

The methylomes observed in co-NECs and CRC adenocarcinomas were far more distinctive of each tumor type than their abovementioned mutational profiles. Co-NECs presented in general lower methylated genomes than CRC tumors in gene regulatory regions, showing very different profiles. Similarly, cells from different differentiation lineages present in the normal intestinal epithelia are governed by a distinctive methylation pattern. We could therefore speculate that the epigenetic fingerprint of a co-NEC is a heritage of a normal cell of origin different from the intestinal cell generating a CRC carcinoma.

Furthermore, key components of central oncogenic pathways such as RTK/KRAS/BRAF/MEK or ILR/JAK/STAT were higher methylated in co-NEC than in CRC, whereas components of the GPCR/PLC/Ca++ signaling were less methylated (Supplementary Figure 2 and 3 and

Supplementary Table 4). Beyond the biological interest of these finding, we observed that the methylation pattern of particular genes central in these oncogenic pathways can determine the response of co-NECs to targeted therapies. This would be the case of *EGFR* gene, which is methylated and repressed in co-NEC resembling the status of melanomas and oppositely to CRC carcinomas where it is less methylated and higher expressed. This is crucial for the response of co-NECs and melanomas to $BRAF^{V600E}$ inhibitors since high EGFR expression has been described as an alternative mechanisms to activate the EGFR/BRAF/MEK pathway and thus an innate mechanisms of resistance in CRC carcinomas[7]. Indeed, our data with PDX confirms the clinical results indicating that CRC do not respond to anti-$BRAF^{V600E}$ drugs alone but in combination with antibodies such as cetuximab bocking EGFR signaling.

On the contrary, melanoma and co-NEC with a methylated and repressed *EGFR* gene showed primary sensitivity to $BRAF^{V600E}$ inhibitors. Moreover, we show how EGFR expression is increased in a co-NEC patient upon acquiring resistance to $BRAF^{V600E}$ blockade with dabrafenib.

In summary, our results indicate that EGFR status is not only essential to predict innate but also acquired resistance to $BRAF^{V600E}$ inhibitors and that the methylation of its regulatory regions would be the underlying mechanisms of regulating its expression in tumors of different origin.

In addition to the efficacy observed in non-small lung cancer[11] and melanoma[12], a recent study in co-NECs showed the first evidence of tumor shrinkage also combining BRAF and MEK inhibitors[6]. Patients were treated based on the prior experience in melanoma and CRC with the BRAF and MEK combination, however no data of BRAF inhibition in monotherapy was provided.

Here we report by the first time that co-NECs with a $BRAF^{V600E}$ mutation could benefit from BRAF inhibitors as monotherapy. Moreover, our results on EGFR indicates that BRAF inhibition should be combined with anti-EGFR antibodies such as cetuximab or panitunumab instead of MEK inhibitors, for an efficient blockade of later acquired resistance.

A more recent study also demonstrate that metastatic CRC patients benefit from a triple inhibition of EGFR, $BRAF^{V600E}$ and MEK in a phase III Beacon trial[13]. Our results suggest that this triple combination could also be beneficial for co-NEC presenting a $BRAF^{V600E}$ mutation. It will be very valuable to generate new PDX models from co-NEC tumors to evaluate the efficacy of such new therapeutic strategies and confirm the relevance of EGFR methylation and expression to predict response to treatment.

Acknowledgements

Authors would like to thank to all patients that allowed to participate in the National GETNE database.

Founding

The current work was supported by an unrestricted grant from the Spanish Task Force for Neuroendocrine and Endocrine Tumors (GETNE-G1101).

REFERENCES

1. Jiao Y, Shi C, Edil BH, de Wilde RF, Klimstra DS, Maitra A, et al. DAXX/ATRX, MEN1, and mTOR pathway genes are frequently altered in pancreatic neuroendocrine tumors. Science. 2011; **331**(6021): 1199-203.
2. Banck MS, Kanwar R, Kulkarni AA, Boora GK, Metge F, Kipp BR, et al. The genomic landscape of small intestine neuroendocrine tumors. The Journal of clinical investigation. 2013; **123**(6): 2502-8.
3. Karpathakis A, Dibra H, Pipinikas C, Feber A, Morris T, Francis J, et al. Prognostic impact of novel molecular subtypes of small intestinal neuroendocrine tumor. Clin Cancer Res. 2016; **22**(1): 250-8.
4. Fernandez-Cuesta L, Peifer M, Lu X, Sun R, Ozretic L, Seidel D, et al. Frequent mutations in chromatin-remodelling genes in pulmonary carcinoids. Nature communications. 2014; **5**: 3518.
5. George J, Lim JS, Jang SJ, Cun Y, Ozretic L, Kong G, et al. Comprehensive genomic profiles of small cell lung cancer. Nature. 2015; **524**(7563): 47-53.
6. Klempner SJ, Gershenhorn B, Tran P, Lee TK, Erlander MG, Gowen K, et al. BRAFV600E Mutations in High-Grade Colorectal Neuroendocrine Tumors May Predict Responsiveness to BRAF-MEK Combination Therapy. Cancer Discov. 2016; **6**(6): 594-600.
7. Prahallad A, Sun C, Huang S, Di Nicolantonio F, Salazar R, Zecchin D, et al. Unresponsiveness of colon cancer to BRAF(V600E) inhibition through feedback activation of EGFR. Nature. 2012; **483**(7387): 100-3.
8. Wang J, Huang SK, Marzese DM, Hsu SC, Kawas NP, Chong KK, et al. Epigenetic changes of EGFR have an important role in BRAF inhibitor-resistant cutaneous melanomas. J Invest Dermatol. 2015; **135**(2): 532-41.
9. Yu G, Wang LG, Han Y, He QY. clusterProfiler: an R package for comparing biological themes among gene clusters. Omics : a journal of integrative biology. 2012; **16**(5): 284-7.
10. Schmittgen TD, Livak KJ. Analyzing real-time PCR data by the comparative C(T) method. Nat Protoc. 2008; **3**(6): 1101-8.
11. Planchard D, Smit EF, Groen HJM, Mazieres J, Besse B, Helland A, et al. Dabrafenib plus trametinib in patients with previously untreated BRAF(V600E)-mutant metastatic non-small-cell lung cancer: an open-label, phase 2 trial. The Lancet Oncology. 2017; **18**(10): 1307-16.
12. Dummer R, Ascierto PA, Gogas HJ, Arance A, Mandala M, Liszkay G, et al. Encorafenib plus binimetinib versus vemurafenib or encorafenib in patients with BRAF-mutant melanoma (COLUMBUS): a multicentre, open-label, randomised phase 3 trial. The Lancet Oncology. 2018; **19**(5): 603-15.

13. Van Cutsem E, Huijberts S, Grothey A, Yaeger R, Cuyle PJ, Elez E, et al. Binimetinib, Encorafenib, and Cetuximab Triplet Therapy for Patients With BRAF V600E-Mutant Metastatic Colorectal Cancer: Safety Lead-In Results From the Phase III BEACON Colorectal Cancer Study. Journal of clinical oncology : official journal of the American Society of Clinical Oncology. 2019; **37**(17): 1460-9.

FIGURE LEGENDS

Figure 1. Mutational profile of co-NEC. A. panel of cancer-related genes was sequenced and mutated cases are indicated in 25 co-NET patients´ tumors. The type of mutation is also detailed. On the right panel, the frequency of cases mutated per each gene is indicated for co-NET and compared with CRC cases studied by TCGA.

Figure 2. Co-NETs respond to BRAF^{V600E} blockade. **A**. Representative images showing the histology of a CRC (CTAX002) and a co-NEC (CTAX012) PDX model and their expression of synaptophysin (SYP). Scale bars: 100 μm. **B**. Both PDX models were treated with the BRAF^{V600E} inhibitor encorafenib and tumor growth is shown. Ten animals were evaluated per each treatment. **** correspond to $p<0.0001$ of an un-paired *t* test with Welch correction comparing the tumor volume at endpoint measurements. **C**. Diagram showing the lesions and histology of a patient presenting an advanced co-NEC with live metastases. Expression of proliferation (Ki67) and NEC differentiation markers (Chromogranin A: CGA and SYP) are shown. Scale bar: 100 μm. **E**. Computed tomography images showing the response and progression of this same patient to BRAF^{V600E} inhibition with dabrafenib. Arrows point major liver lesions that are also delineated.

Figure 3. **Co-NECs show a distinctive methylome**. **A.** A principal component dot plot showing the differences of methylation profiles between co-NECs and CRC. **B**. A volcano plot showing significant differences in methylation status of CpGs island in co-NECs and CRC adenocarcinomas. **C.** A hierarchical cluster showing two different clusters of methylation profiles in co-NET and CRC. The type of genome regions is also indicated. **D**. From the list of genes differentially methylated in co-NECs versus CRC we performed Gene Set Enrichment Analyses (GSEA) using Broad Institute online tools. A list of gene sets significantly enriched in co-NEC versus CRC is shown indicating the number of genes per set (size) and their enrichment score (ES). **E**. GSEA plots showing enrichment of particular gene sets when comparing genes differentially methylated in co-NEC versus CRC cases. p values are indicated as well as particular genes in the leading edge.

Figure 4. *EGFR* gene is methylated and repressed in co-NECs conferring innate sensitivity to BRAF*V600E* inhibition. A. Methylation pattern of *EGFR* gene in co-NEC, CRC and melanoma tumors. **** correspond to p<0.0001 by an unpaired *t* test with Welch correction **B**. Histology showing the expression of EGFR in a representative co-NEC and a CRC carcinoma. **C**. Dot plot representing the level of EGFR protein expression measured by IHC in co-NETs and CRC carcinomas. *** correspond to p<0.001 by an unpaired *t* test with Welch correction. **D**. Histology showing the expression of EGFR in a co-NEC tumor at baseline or after patient progressing to $BRAF^{V600E}$ inhibition with dabrafenib. **B** and **D**. Scale bars: 100 μm. **E**. Column plot representing the quantification of IHC shown in panel E. **F**. Both PDX models (CRC-CTAX002 and Co-NEC-CTAX012) were treated with the $BRAF^{V600E}$ inhibitor encorafenib alone or in combination with Cetuximab and tumor growth is shown. Ten animals were evaluated per each treatment. **** correspond to p<0.0001 of an un-paired t test with Welch correction comparing the tumor volume at endpoint measures. **G**. mRNA expression of EGFR gene in three tumor xenografts from each indicated PDX model. **H**. The basal levels of EGFR and phospho-EGFR (p-EGFR) proteins were measured by Western blot in three tumor xenograft from each indicated PDX model. Tubulin was used as loading control.

FIGURE 1

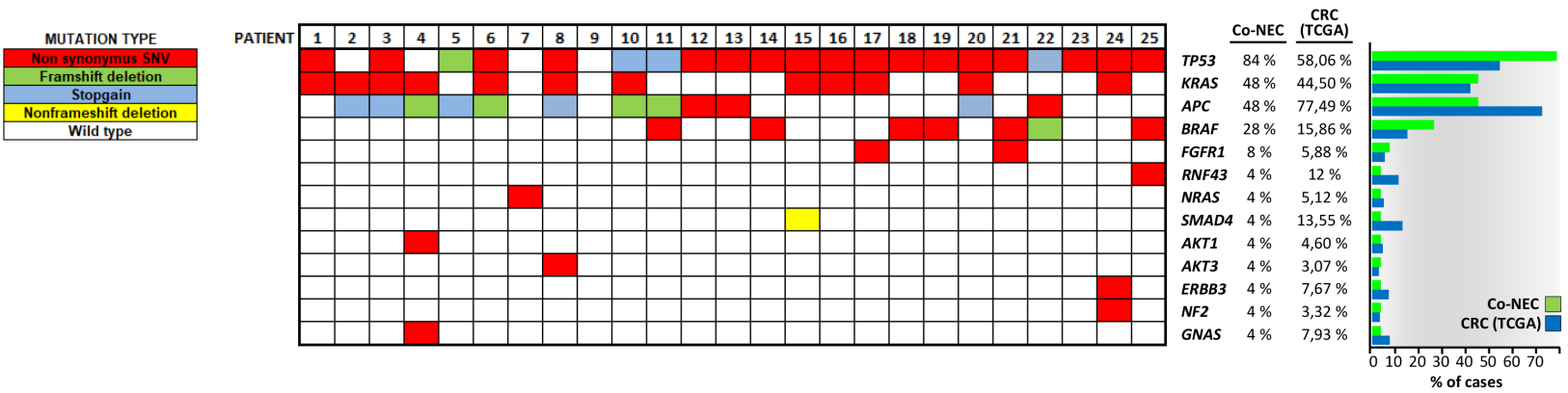

FIGURE 2

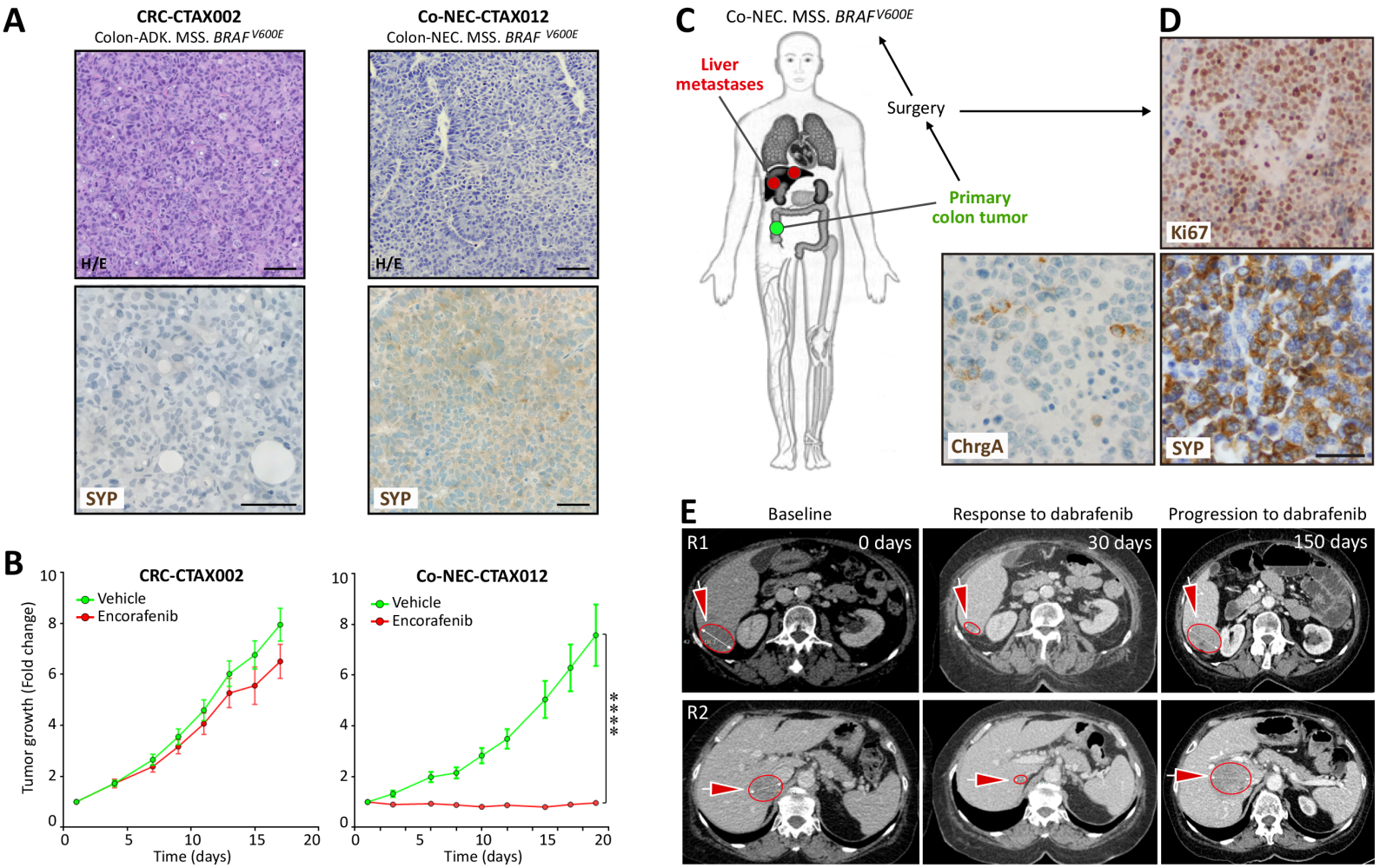

FIGURE 3

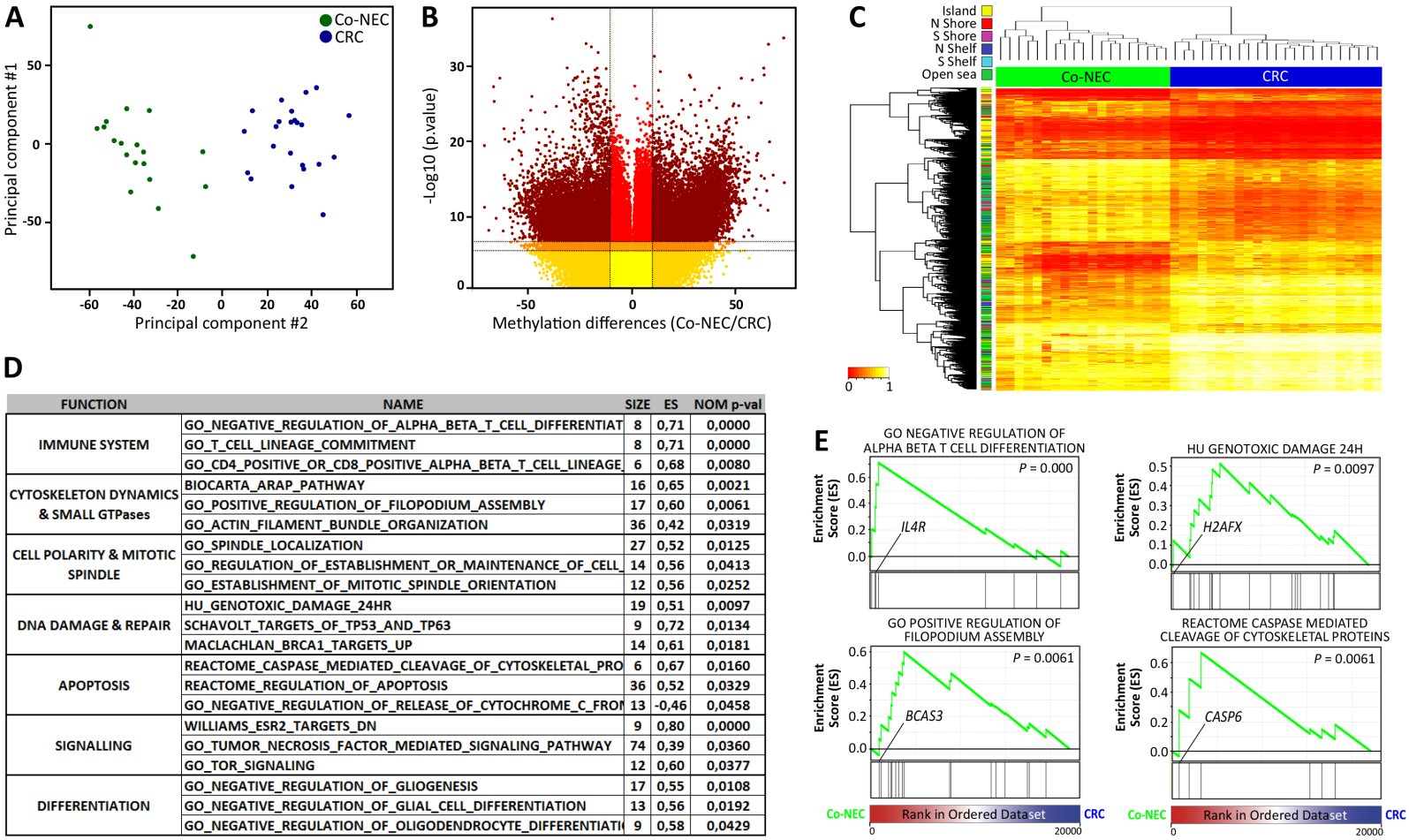

D

FUNCTION	NAME	SIZE	ES	NOM p-val
IMMUNE SYSTEM	GO_NEGATIVE_REGULATION_OF_ALPHA_BETA_T_CELL_DIFFERENTIAT	8	0,71	0,0000
	GO_T_CELL_LINEAGE_COMMITMENT	8	0,71	0,0000
	GO_CD4_POSITIVE_OR_CD8_POSITIVE_ALPHA_BETA_T_CELL_LINEAGE	6	0,68	0,0080
CYTOSKELETON DYNAMICS & SMALL GTPases	BIOCARTA_ARAP_PATHWAY	16	0,65	0,0021
	GO_POSITIVE_REGULATION_OF_FILOPODIUM_ASSEMBLY	17	0,60	0,0061
	GO_ACTIN_FILAMENT_BUNDLE_ORGANIZATION	36	0,42	0,0319
CELL POLARITY & MITOTIC SPINDLE	GO_SPINDLE_LOCALIZATION	27	0,52	0,0125
	GO_REGULATION_OF_ESTABLISHMENT_OR_MAINTENANCE_OF_CELL_	14	0,56	0,0413
	GO_ESTABLISHMENT_OF_MITOTIC_SPINDLE_ORIENTATION	12	0,56	0,0252
DNA DAMAGE & REPAIR	HU_GENOTOXIC_DAMAGE_24HR	19	0,51	0,0097
	SCHAVOLT_TARGETS_OF_TP53_AND_TP63	9	0,72	0,0134
	MACLACHLAN_BRCA1_TARGETS_UP	14	0,61	0,0181
APOPTOSIS	REACTOME_CASPASE_MEDIATED_CLEAVAGE_OF_CYTOSKELETAL_PRO	6	0,67	0,0160
	REACTOME_REGULATION_OF_APOPTOSIS	36	0,52	0,0329
	GO_NEGATIVE_REGULATION_OF_RELEASE_OF_CYTOCHROME_C_FROM	13	-0,46	0,0458
SIGNALLING	WILLIAMS_ESR2_TARGETS_DN	9	0,80	0,0000
	GO_TUMOR_NECROSIS_FACTOR_MEDIATED_SIGNALING_PATHWAY	74	0,39	0,0360
	GO_TOR_SIGNALING	12	0,60	0,0377
DIFFERENTIATION	GO_NEGATIVE_REGULATION_OF_GLIOGENESIS	17	0,55	0,0108
	GO_NEGATIVE_REGULATION_OF_GLIAL_CELL_DIFFERENTIATION	13	0,56	0,0192
	GO_NEGATIVE_REGULATION_OF_OLIGODENDROCYTE_DIFFERENTIATI	9	0,58	0,0429

FIGURE 4

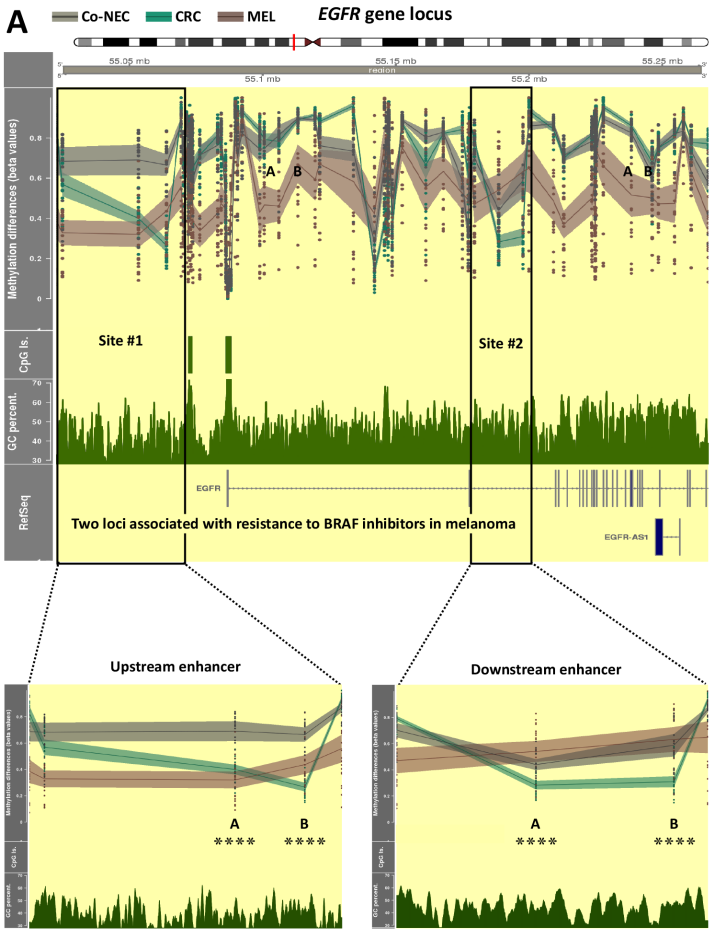

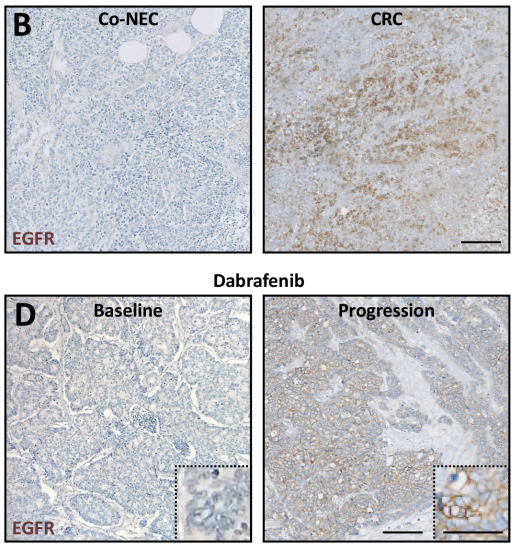

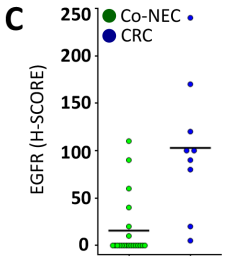

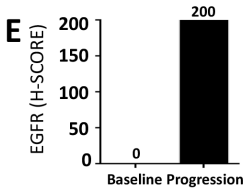

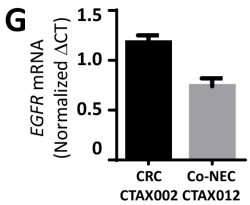

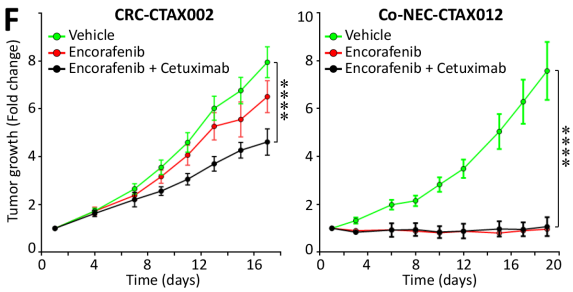

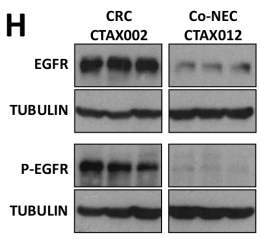

AACR American Association for Cancer Research

Clinical Cancer Research

Epigenetic EGFR gene repression confers sensitivity to therapeutic BRAFV600E blockade in colon neuroendocrine carcinomas

Jaume Capdevila, Oriol Arqués, Jose Ramon Hernandez Mora, et al.

Clin Cancer Res Published OnlineFirst October 31, 2019.